

## CONSTRUCTION OF A HIGH CURRENT RFQ FOR ADS STUDY

S.N. Fu, S.X. Fang, X.L. Guan<sup>1</sup> H.F. Ouyang, T.G. Xu, Z.H. Zhang, J.M. Qiao, W.W. Xu, Z.H. Lou, Q.C. Yu, J. Li, X.A. Xu, Y. Yao, H.S. Zhang, K.Y. Gong, R.J. Shao<sup>2</sup>, X.Y. Wang<sup>2</sup> Z.Y. Guo<sup>3</sup>

J.X. Fang<sup>3</sup>, A. Pisent<sup>4</sup>, G. Lamanna<sup>4</sup>, M. Comunian<sup>4</sup>, A. Palmieri<sup>4</sup>

IHEP, Institute of High Energy Physics, Beijing 100049, China

<sup>1</sup>CIAE, China Institute of Atomic Energy, Beijing 102413, China

<sup>2</sup>Shanghai Kelin Accelerator Technology Development Co. Ltd., Shanghai 200240, China

<sup>3</sup>IHIP, Institute of Heavy Ion Physics, Peking University, Beijing 100871, China

<sup>4</sup>INFN-LNL, I-35020, Legnaro, Italy

### Abstract

A high current proton RFQ accelerator has been constructed in China for the basic study of Accelerator Driven Subcritical System. The ADS project is supported by a national program and aimed at the development of clean nuclear energy to meet of the rapid growth of the nuclear power plants in China. The 3.5MeV RFQ accelerator has been fabricated and installed. The beam commissioning with an ECR ion source showed a nice performance of the RFQ with a transmission rate about 92% in the initial test at an injection current of 44mA. This paper presents the recent progress in the construction and commissioning of the RFQ accelerator.

### INTRODUCTION

China will speed up the development of nuclear power to meet the energy demand of the rapid and continuing economic growth. It is foreseen that 40GW nuclear power will be developed by 2020 in China (about 80% of the present France nuclear power). Accelerator Driven Subcritical system (ADS) is recognized as one of the best options of fission nuclear power source. A basic research program of ADS was lunched in 2000 under the support of the Ministry of Science and Technology, China [1]. In this program, a high-current proton RFQ accelerator has been constructed at IHEP. In this paper, we will describe the major design features of the RFQ in the second section. Then, manufacture of the RFQ cavity will be outlined in the third section. The fourth section will show cavity tuning process and results. Finally the high power conditioning and the initial beam commissioning in recent will be presented in the last section.

### DESIGN FEATURES OF THE RFQ [2]

The major parameters of the RFQ are listed in Table 1. This 3.5MeV RFQ is about  $5\lambda$  long. To address the longitudinal field stability, it is separated into two resonantly coupled segments. Each segment consists of two technological modules of nearly 1.2m in length. On each module there are 16 tuners distributed on the 4 quadrants for frequency and field tuning. Dipole

stabilizer rods on both the end plates and the coupling plate are applied. As a high-duty machine with 6% duty factor in the first phase and eventually to 100% in future, cooling water is necessary to keep the thermal stability. There are 20 cooling channels on the cavity body in each module: 8 on the vane and 12 on the wall. The water temperature on the vane and wall can be independently adjusted for resonance control of the cavity in high power operation. Eight vacuum ports are designed on the first and fourth modules, respectively, and eight RF feed ports are located on the second and third modules. However, only half of the vacuum and power ports are used for the present 6% duty operation and other ports will be used when the RFQ is operated at a higher duty factor in the future Four vane-wall pieces are brazed to form a cavity for both RF and vacuum seals.

Table 1: RFQ Major Parameters

Input Energy	75keV
Output Energy	3.5MeV
Peak Current	50mA
Structure Type	4 vane
Duty Factor	6%-100%
RF Frequency	352.2MHz
Maximum $E_s$	33MV/m
Beam Power	170kW
Structure Power	420kW
Total Power	590kW
Total Length	4.75 m

### MANUFACTURE OF THE CAVITY

A cavity is composed of four pieces: two vertical major vanes and two horizontal minor vanes. Prior to the cavity manufacture, we had a series of R&D tests to master the key technologies in each important fabrication step. A short section was first made for high accuracy machining test, especially the form cutter test. And then a full size test cavity was worked out for brazing demonstration and deep drill test of the cooling channels.

Deep drill of the cooling channels of 1.2m long on the roughly machined pieces resulted a large deviation (about 2-3mm) from end to end for a single channel. But fortunately, the other channels in the same piece had

almost the same amount of deviation in the same direction. So the second rough machining was conducted in line with the systematic deviation, and thus the resulted deviation is almost within the tolerance.

Form cutter is a key technology for vane modulation fine machining. We tested a lot and failed many times during one and half years, and finally we successfully made a cutter with both a high curvature-radius accuracy and a low cutting abrasion. In fact, we used only a single cutter for all fine machining of the vanes of the RFQ (16 pieces of 1.2m long vane).

After fine machining, each piece was measured with a CMM. The measured modulation curve was compared with design curve, and some errors were detected. Figure 1 plots a small section of the curves. It can be seen there is about  $30\mu\text{m}$  amplitude error in this section.

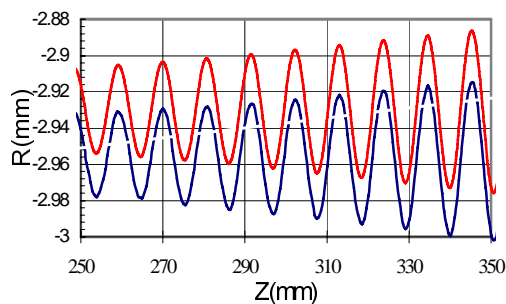


Figure 1: Comparison of the measured and designed vane modulation curve.

The four pieces were assembled to form a cavity. The position adjustment of the two horizontal vanes in the assembly step gives a chance to compensate the machining errors. Bead pull measurement of the cavity field in the four quadrants and ping gauge measurement of the geometric distance of the neighbour vanes guided the horizontal minor vane adjustment. The aims of the adjustment are to make the field component of dipole mode as low as possible, and the resonant frequency of the four modules as close as possible. For example, we reduced the dipole component from 14% in the initial assembly to 3% with flushed tuners. Tuning the field by aluminium movable tuners demonstrated the cavity module could be easily tuned to the design frequency and much lower dipole component of 1%.

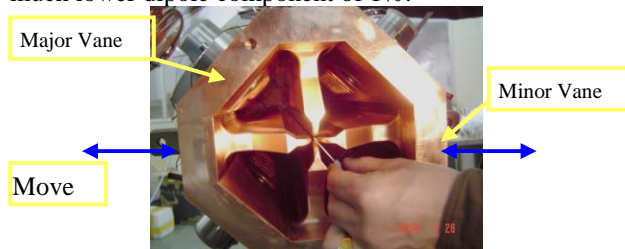


Figure 2: Geometrical measurement of the distance between neighbour vanes by a series of pin gauges for position adjustment of the two horizontal minor vanes.

The assembled cavity was brazed in a vertical hydrogen furnace at temperature around  $830^{\circ}\text{C}$  with silver-copper filler. The braze of a cavity was achieved

by two stages: in the first stage the assembled four pieces and the stainless steel end flanges were brazed together to form a vacuum tight RF cavity (Figure 3); then in the second stage all tuner flanges, water ducts, vacuum grill bodies (Figure 4) on the 1<sup>st</sup> and 4<sup>th</sup> module or RF power feed port flanges on the 2<sup>nd</sup> and 3<sup>rd</sup> module were assembled onto the cavity and then brazed (Figure 5). The key issues in the braze are how to keep all of the 266 brazing seams vacuum tight, to remain no filler on the inner surface of the cavity and to guarantee sufficient small deformation of the cavity shape in the periodic thermal effects. We made vacuum leakage check and bead pull measurement before and after each braze stage to verify these requirements had been satisfied. For the 1<sup>st</sup> and 4<sup>th</sup> modules, an additional requirement is the vacuum grill bodies should be penetrates into the inner surface 0.7mm to compensate for the frequency perturbation of the grill openings. It is not easy to meet this requirement in the vertical braze. In fact, two vacuum bodies on the 4<sup>th</sup> module were found almost no penetration after braze, and thus, a repairing braze was performed to correct the insertion depth.

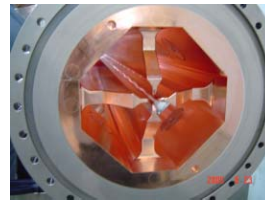


Figure 3: RFQ cavity after the first braze.



Figure 4: Vacuum grill body.

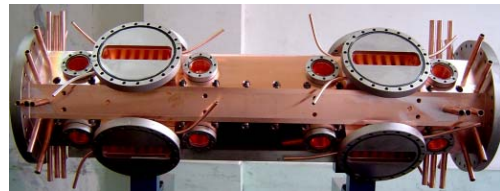


Figure 5: RFQ cavity after the second braze.

## INSTALLATION AND TUNING

Four manufactured modules were installed together for frequency and field tuning. A laser tracker was applied for the alignment of the four modules. The achieved alignment accuracy is about  $30\mu\text{m}$ . Some movable aluminium tuners and aluminium end plates and coupling plate with dipole stabilizer rods were also installed. For simplicity the dipole rods on the coupling plate had a fixed length according to our 3D modelling and the previous experiment data from the model cavity. The rod length on the end plates was variable.

A bead of 6mm in diameter was used for field perturbation measurement. S21 phase data were taken into a vector network analyser as the bead went through the cavity from one end to another end. The bead was located nearby the two neighbour vanes for electrical field measurement, and thus it had no interference with the coupling plate. We moved the same bead around the

four quadrants instead of using four beads. A tuning code developed on LabView platform analysed the measured field data in the four quadrants and gave an instruction of the tuners' insertion in the next iteration. After several iterations, a nice field was achieved with a flat quadrupole mode and small dipole mode, as shown in Figure 6. It can be observed from the plot, the quadrupole flatness is better than 1% in maximum, and the dipole component is within 2% in maximum.

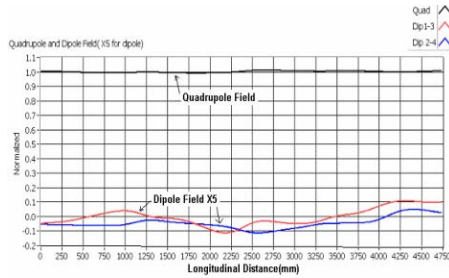


Figure 6: The quadrupole field and dipole field (5 times magnified) after tuning.

Then these movable aluminium tuners were replaced with the fixed copper tuners by several batches. Because the aluminium tuners were not exactly the same as the copper ones, the remaining movable tuners in each batch were tuned to compensate for the difference, but not all. Consequently, the flatness of quadrupole becomes 2% in maximum and dipole component keeps almost the same after the replacement.

### CONDITIONING AND COMMISSIONING

The RF power source and the waveguide come from CERN. It was a CW RF power source of 352.2MHz/1.2MW, decommissioned from LEP II. The modulator from CERN worked in ramping mode for LEP II. To adapt to our RFQ's square pulse mode at various duty factors, some necessary modifications of the system have been made [3]. As we have only obtained the waveguide part of the waveguide-coaxial transition, we designed and fabricated four coaxial lines with a loop coupler and a ceramic window for each, as shown in Figure 7. RF power transmission and feed system were set up for high power conditioning of the RFQ cavity.



Figure 7: Coaxial line and ceramic window at transition.

Cavity conditioning was arranged in three steps: lower peak power at a high duty without cooling water for outgassing conditioning of the surface in the first step (Figure 8); and then high peak power at a low duty for the spark conditioning of the surface in the second step; finally high power at a high duty. We reached a cavity

input power of 440kW at a duty factor of 7%. In this high power run, the effect of 0.2°C water temperature difference between the vane and wall can be observed. After the high power conditioning the static vacuum reached 2.5E-6 Pa while it had been 4.6E-5Pa before conditioning.

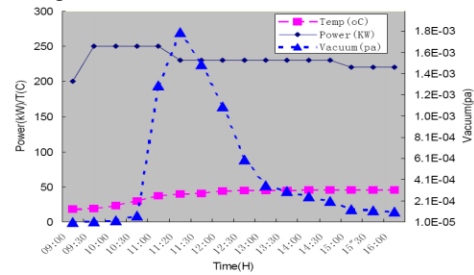


Figure 8: The cavity temperature and vacuum variation with input power during low-power high-duty conditioning.

The entrance end of the RFQ was opened for connection with the ECR proton source for beam commissioning. It was found that there was a strong sparking trace on the vane tip surfaces and the dipole rods. The trace had almost the same length as that of the dipole rod. More deeply inside the cavity, there almost no sparking trace could be observed. So it can be inferred that the major sparking happened between the vanes and the dipole rods.

Beam commissioning started in recent at a low beam duty (0.5%) but a higher RF duty (1.5%). As an initial result after a short time tuning of the ion source and solenoids in the LEBT, we reached a transmission rate of 92% with an input beam of 44mA. Figure 9 shows the beam pulses measured by the two ACCTs at the input end (blue curve) and the output end (yellow curve). Now we are pushing forward to a higher beam duty.

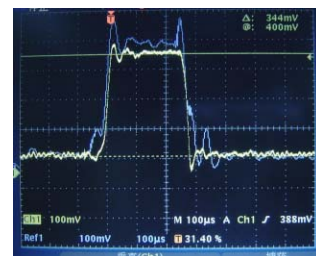


Figure 9: Beam current signals from the ACCTs.

### ACKNOWLEDGEMENTS

We are very grateful to K. Hubner, H. Frischholz and their colleagues at CERN for their kind support in RF power source. We thank B.H. Choi and Y.S. Cho of KAERI for their friendly cooperation. The fruitful discussions with J. Stapels, D. Li and S. Virostek of LBL are highly appreciated.

### REFERENCES

- [1] S.X.Fang, Current Status of ADS R&D in China, <http://www.kaeri.re.kr/npet/WS-9/KOMAC/main.htm>
- [2] Shinian Fu et al., Proc. of LINAC'02, p.154.
- [3] Zhang Zonghua et al., Proc. of LINAC04, THP-47.